3-D-Printed Dielectric Resonator Antenna Arrays Based on Standing-Wave Feeding Approach

Ayman A. Althuwayb, Kerlos A. Abdalmalak, *Student Member, IEEE*, Choon S. Lee, *Senior Member, IEEE*, Gabriel Santamaría-Botello, Luis E. García-Castillo, *Member, IEEE*, Daniel Segovia-Vargas, *Member, IEEE*, and Luis E. García-Muñoz

***Abstract*—A novel feeding method for a dielectric resonator array antenna is introduced. Unlike in a corporate feed network, power dividers or quarter-wave transformers are not needed in the new feeding scheme as the design is based on the standing-wave concept. Consequently, the feed network is greatly simplified, and undesired spurious radiation in the feeding network is minimized. The simulated and measured results are in good agreement. A 3-D printer is utilized where the entire array structure is fabricated as a single piece with a dielectric material of polylactic acid. The 3-D printer provides a cost-efficient, simple, and rapid manufacturing process.**

***Index Terms*—Array antenna feed, dielectric resonator antenna (DRA), planar array, standing wave, 3-D printer.**

I. Introduction

DIELECTRIC resonator antennas (DRAs) have recently been attracting attention in the literature due to the fact that they have a number of advantageous features, including excitation and fabrication easiness, low weight, low loss, and versatility [1]–[3]. Although DRAs have been widely used for various applications at microwave frequencies [4]–[6], they typically exhibit relatively low gain [7], which unfavorably affects the DRA advantages. One straightforward approach to enhance the gain is to assemble DRAs to form an array that is capable of achieving relatively high gains. Corporate feed networks are commonly utilized in DRA arrays [8]–[10]. A conventional traveling-wave corporate-fed network consists of numerous microstrip transmission lines to feed the array elements equally in magnitude and phase for high-gain applications. With such a feeding scheme, losses in the transmission lines can be substantial, especially at higher frequencies [11], [12], due to microstrip discontinuities in the feeding network [13]. Thus, eliminating them is required to achieve better efficiencies for the high-frequency applications [14], [15]. As an alternative feeding mechanism, a substrate-integrated waveguide (SIW) has been utilized to feed DRA arrays [16]–[18]. Although SIW structures exhibit relatively high radiation efficiency, it is likely to have considerable leakage losses that, in turn, will lead to wave attenuation, especially in large planar array structures [19], [20]. Another feeding scheme to excite a DRA array is utilizing a dielectric image guide (DIG) that feeds RF power from the launcher to the resonators [21], [22]. In this feeding method, a considerable back radiation is observed because the aperture radiates in both directions. Additionally, rectangular waveguides are required to launch the DIG, which adds to the array size and the overall cost [23]. In this letter, a novel configuration for DRA arrays is proposed, in which a formation of the standing wave within the array structure is proven to be an effective excitation mechanism to alleviate such mentioned losses. A standing wave is created by two waves traveling in opposite directions. A cavity can be in a resonant state when the multiple bouncing waves become constructively interfered [24], [25]. The antenna-element design process is given in Section II. The simulated and measured results of array antennas are presented in Section III with comparison to other DRA feeding approaches, followed by concluding remarks in Section IV.

Manuscript received August 16, 2019; revised August 31, 2019; accepted September 1, 2019. Date of publication September 6, 2019; date of current version October 4, 2019. This work was supported by Comunidad de Madrid under Projects S2018/NMT-4333 MARTINLARA-CM and TEC2016-80386-P. *(Corresponding author: Ayman Abdulhadi Althuwayb.)*

A. A. Althuwayb is with the Electrical Engineering Department, Jouf University, Sakaka 72388, Saudi Arabia (e-mail: aaalthuwayb@ju.edu.sa).

K. A. Abdalmalak is with the Signal Theory and Communications Department, Carlos III University of Madrid, Madrid 28911, Spain, and also with the Electrical Engineering Department, Aswan University, Aswan 81542, Egypt (e-mail: Kerlos.atia@alumnos.uc3m.es).

C. S. Lee is with the Electrical and Computer Engineering Department, Southern Methodist University, Dallas, TX 75205 USA (e-mail: csl@lyle.smu.edu).

G. Santamaría-Botello, L. E. García-Castillo, D. Segovia-Vargas, and L. E. García-Muñoz are with the Signal Theory and Communications Department, Carlos III University of Madrid, Madrid 28911 Spain (e-mail: gsant@tsc.uc3m.es; luise@tsc.uc3m.es; dani@tsc.uc3m.es; legarcia@tsc.uc3m.es).

Digital Object Identifier 10.1109/LAWP.2019.2939734

II. Antenna Element

The design process starts with a rectangular DRA (RDRA) where a TE_{115} mode is excited at $f_r = 5.6\,\mathrm{GHz}$ to get a higher gain than those of lower order modes. The initial dimensions of the RDRA are obtained using the following equation along with the design curves provided in [7]:

$$L_r = \frac{Fc}{2\pi f_0 \sqrt{\varepsilon_r}} \tag{1}$$

where L_r represents the RDRA length normal to the feeding line, c is the speed of light, f_0 is the resonant frequency, ε_r is the relative permittivity of the dielectric resonator, and F is the normalized frequency obtained from the referenced curves [7]. Then, the height of the RDRA is further increased for the TE_{115} mode. The optimum dimensions of the RDRA are $L_{r1} = 25\,\mathrm{mm}$, $W_{r1} = 25\,\mathrm{mm}$, and $H_{r1} = 60.5\,\mathrm{mm}$, and it is

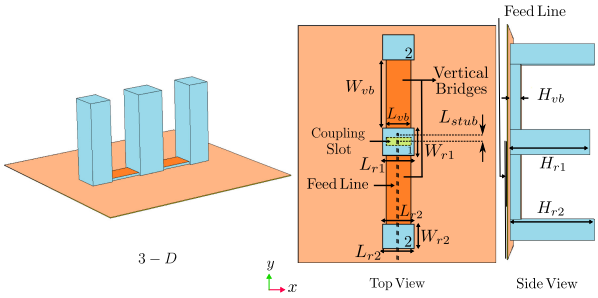

Fig. 1. Three-element standing-wave linear DRA array.

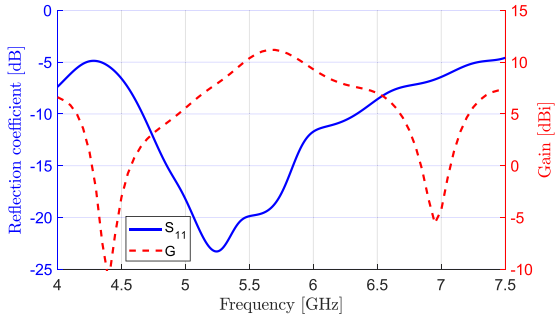

Fig. 2. Simulated S_{11} and gain vs frequency of the linear DRA array.

made of PLA material with relative permittivity $\varepsilon_r = 2.5$ and loss tangent 0.005 [26], [27]. It is mounted at the center of Arlon 25 N substrate with relative permittivity $\varepsilon_{\text{sub}} = 3.38$, loss tangent 0.0015, and a height of 0.508 mm. The antenna is fed with a coupling slot engraved on the top layer (ground plane) under the DRA element and a transmission line attached to the bottom surface of the substrate. The input impedance of the antenna can easily be matched by varying the slot dimensions and the matching stub length (L_{stub}), which is defined from the slot center to the end of the microstrip line (open-ended).

High-Frequency Structure Simulator (HFSS) [28] is used to obtain the simulated results. At the resonant frequency $f_r = 5.6$ GHz, excellent impedance matching is achieved with a wide impedance bandwidth of about 26.5%. The antenna produces a peak gain of 8.5 dBi.

III. Array Design and Measurements

A. Three-Element Linear Array

The proposed excitation mechanism for DRA arrays is based on the concept of standing wave. It is important to connect the array elements with bridges so that a standing wave is formed within the array cavity. Low-profile dielectric bridges are introduced between the array elements, as depicted in Fig. 1. Due to the variation in the boundary conditions between the central element (labeled as 1) and other elements (labeled as 2), the width (W_{r2}) and height (H_{r2}) of the latter are further optimized for maximum gain. The optimum dimensions of the radiating elements (number 2) are $L_{r2} = 25$ mm, $W_{r2} = 20.75$ mm, and $H_{r2} = 65$ mm. The width of the low-profile dielectric bridges (W_{vb}) is chosen so that the spacing along the y-axis between neighboring elements is approximately one and a half guided wavelengths (λ_g) due to the fact that the fields at the front and back walls (normal to the feedline) of the radiating resonators have about maximum magnitudes with opposite phases.

The dimensions of the bridges are $L_{vb} = 20$ mm, $W_{vb} = 65$ mm, and $H_{vb} = 8$ mm, and they are made of the same material as of the radiating elements. They are covered by metal plates on both the bottom side (ground plane of the Arlon substrate) and the upper side (metallic covers) to confine the wave excitations between the conducting surfaces. The sidewalls of the bridges are kept open for design convenience and easy fabrication. The contribution of the openings to the far fields is relatively small since the dominant electric-field component for radiation has phase reversals within each sidewall surface. The situation is similar to the case of the nonradiating edges in a microstrip antenna [29]. Additionally, the heights of the bridges are much smaller than those of the other radiation structures in the array, affecting the radiated fields far less.

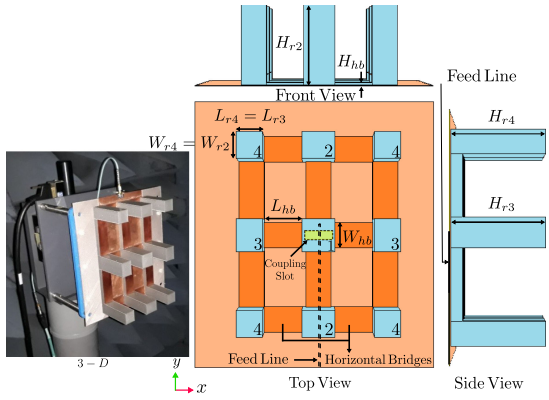

Fig. 3. A 3 × 3 standing-wave planar array.

The simulated reflection coefficient shows excellent impedance matching over a wide frequency range from 4.7 to 6.3 GHz as shown in Fig. 2. A maximum realized gain of 11.2 dBi is observed with a 3 dB bandwidth of 16% from 5.27 to 6.17 GHz. Such gain enhancement justifies the standing-wave feeding technique for the linear array. The standing-wave feed scheme is also applicable to arrays with lower order modes in the dielectric radiating elements including the fundamental mode of TE_{111}, where most geometrical parameters remain the same. For example, in the array designs with two different modes of TE_{115} and TE_{111}, the only difference is that the height of the dielectric elements of TE_{111} is about one-third of that of TE_{115} while all other dimensions are the same. The gain with TE_{111} is reduced by 4.5 dBi compared with that of TE_{115}, which is in line with the theoretical evaluation of the two cases [30].

B. Nine-Element Planar Array

To form a 3 × 3 planar DRA array, the proposed linear array configuration is duplicated twice. Six dielectric bridges horizontally connecting each element with its neighboring ones are introduced, as illustrated in Fig. 3. Since the elements on the array edges are not the same as the central element in terms of electromagnetic interaction, the dimensions of the peripheral elements have to be adjusted to achieve optimum gain. The length of element number 3 (L_{r3}), as well as the width of element

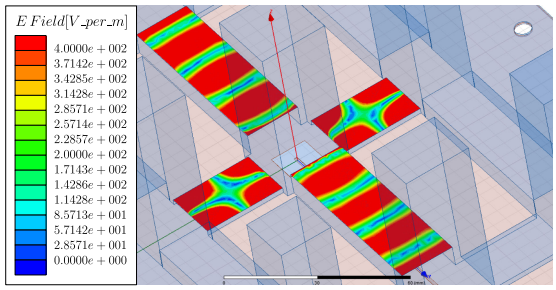

Fig. 4. Electric field distribution within the bridges.

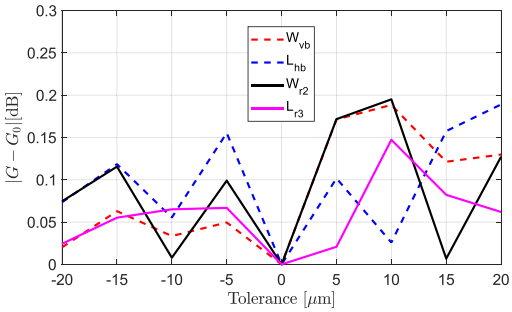

Fig. 5. Sensitivity effect of geometrical parameters on the gain of the proposed array.

number 2 (W_{r2}), is slightly optimized. The optimized dimensions of the radiating elements are $L_{r4} = L_{r3} = 19.75$ mm, $W_{r4} = W_{r2} = 20$ mm, and $H_{r4} = H_{r3} = H_{r2} = 65$ mm. The spacing along the x-axis between neighboring elements is approximately a half-guided wavelength (λ_g) due to the fact that the fields at the right and left walls (parallel to the feedline) of the radiating elements for endfire radiation have almost the same magnitudes but opposite phases. Fig. 4 shows the modes excited in the bridges, which are $\mathrm{TEM_y}$ and $\mathrm{TE_{x10}}$, to form a standing wave in the y-direction and x-direction, respectively. The optimized dimensions of the horizontal bridges are $L_{hb} = 30$ mm, $W_{hb} = 20$ mm, and $H_{hb} = 2$ mm. As in the linear array, the array excitation is simplified to feed only the central element.

The design tolerance of the proposed planar standing-wave array is investigated prior to fabrication. A BCN3D Sigma 3-D printer was utilized to fabricate the prototype, which has an accuracy of ± 20 μm. The effect of variation of the dimensions on the antenna gain is shown in Fig. 5. For simplicity, the effect of only four main parameters that have considerable influence on the array gain is shown. Negligible gain variations are less than ± 0.2 dBi, which corresponds to an error of $\pm 4.5\%$.

The simulated and measured reflection coefficients and gains are shown in Fig. 6. The measurements show a very large impedance bandwidth of 35% with a maximum gain of about 15 dBi. It is worth noting here that, when the metallic covers over the bridges are removed, the resultant gain significantly drops (around 5.5 dBi) although the reflection coefficient remains almost the same. Such reduced gain is due to altered field distribution within the array structure after removing the metallic covers over the bridges, which signifies the roles of the bridges in the standing-wave array design. The measured radiation patterns are in good agreement with the simulated as shown in Fig. 7. The measured cross-polarization levels are relatively low. The

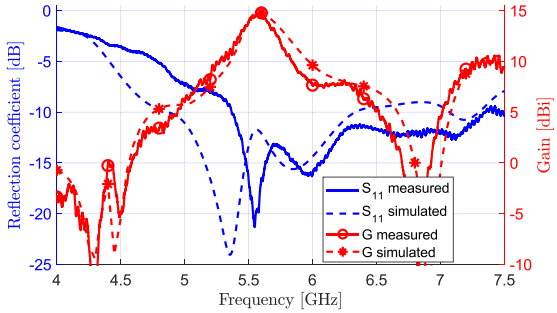

Fig. 6. Simulated and measured S_{11} and gain vs. frequency of the 3×3 standing-wave DRA array.

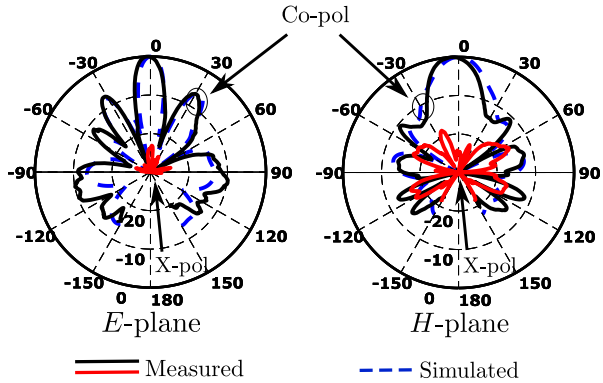

Fig. 7. Simulated and measured normalized radiation pattern of the 3×3 standing-wave DRA array at 5.6 GHz.

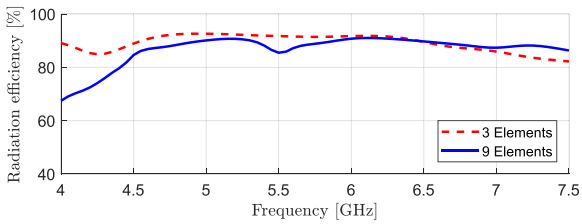

Fig. 8. Simulated radiation efficiency as a function of frequency for both three- and nine-element standing-wave DRA arrays.

radiation efficiency is better than 90% for both the linear and planar array near the resonant frequency (Fig. 8). Table I presents a comparison of the proposed standing-wave feeding method with other state-of-the-art techniques for DRA arrays. The proposed feeding technique has three main attractive characteristics. First, the high and almost constant radiation efficiencies, $92 \pm 1\%$ for the linear array and $88 \pm 3\%$ for the planar array, compare favorably with those of the recently reported feeding schemes [10], [16], [21].

Second, from the design complexity and cost point of view, the proposed feeding scheme offers a much more simplified feeding network compared to other available methods as the proposed scheme needs neither any tapered waveguide and transitions as in DIG, nor hundreds of metallic vias as in SIW, nor power dividers/quarter-wave transformers as in corporate feeds. Moreover, the entire proposed structure is fabricated as a single piece with a 3-D printer, and the alignment process of each individual resonator is avoided. Consequently, the fabrication cost is substantially reduced. Finally, from the gain point of view, it can be seen from Table I that the currently presented feeding

TABLE I
COMPARISON BETWEEN THE PROPOSED SOLUTION AND STATE-OF-THE-ART DRA FEEDING TECHNIQUES

Ref./ year	Feeding techniques	No. of elem.	Gain (dBi)	Impedance and 3dB gain bw (%)	Rad. eff. (%)
Proposed linear array	Standing-wave	3	11.2	15	92 ± 1
[10]/2018	Corporate	4	10	7	86 ± 3
[31]/2017	Separated-layer for the feed lines	4	10.5	12	-
Proposed planar array	Standing-wave	9	15	7	88 ± 3
[16]/2018	SIW	8	13.55	6.3	80 ± 5
[21]/2010	DIG	7	7.61	10	68 ± 4
[21]/2010	DIG	15	12.46	15	74 ± 11

provides higher gain with even a smaller number of elements compared to the other standard feeding techniques.

IV. CONCLUSION

In this letter, a novel feeding technique for DRA arrays based on the formation of a standing wave within the array cavity is introduced. The proposed designs offer a simplified feeding network with a single conventional aperture-coupled scheme that feeds only one array element (in this case, the central dielectric slab). All other radiating elements are excited by the central dielectric resonator through a high-order standing wave formed within the antenna cavity with a number of bridges. Since the array antenna is printed as a single structure, the alignment problem of array elements is eliminated and, hence, easy fabrication process results. Good agreement between the simulated and measured results has been observed. For the nine-element planar array, relatively high radiation efficiency of nearly 90% was obtained over a 3 dB gain bandwidth of 7% with a measured peak gain of about 15 dBi.

ACKNOWLEDGMENT

The authors would like to acknowledge Dr. K. W. Leung of City University of Hong Kong for his valuable discussion and comments.

REFERENCES

[1] K. W. Leung, E. H. Lim, and X. S. Fang, "Dielectric resonator antennas: From the basic to the aesthetic," *Proc. IEEE*, vol. 100, no. 7, pp. 2181–2193, Jul. 2012.

[2] A. Petosa and A. Ittipiboon, "Dielectric resonator antennas: A historical review and the current state of the art," *IEEE Antennas Propag. Mag.*, vol. 52, no. 5, pp. 91–116, Oct. 2010.

[3] A. Petosa, *Dielectric Resonator Antenna Handbook*. Norwood, MA, USA: Artech House, 2007.

[4] K. A. Abdalmalak *et al.*, "Microwave radiation coupling into a WGM resonator for a high-photonic-efficiency nonlinear receiver," in *Proc. 48th Eur. Microw. Conf.*, Sep. 2018, pp. 781–784.

[5] S. K. K. Dash, T. Khan, and B. K. Kanaujia, "Circularly polarized dual facet spiral fed compact triangular dielectric resonator antenna for sensing applications," *IEEE Sensors Lett.*, vol. 2, no. 1, pp. 1–4, Mar. 2018.

[6] E. H. Lim and K. W. Leung, "Novel application of the hollow dielectric resonator antenna as a packaging cover," *IEEE Trans. Antennas Propag.*, vol. 54, no. 2, pp. 484–487, Feb. 2006.

[7] K. Luk and K. Leung, *Dielectric Resonator Antennas* (series Antennas S). Baldock, U.K.: Research Studies Press, 2003.

[8] L. N. Zhang, S. S. Zhong, and S. Q. Xu, "Dielectric resonator antenna element and subarray with unequal cross-stub," *Microw. Opt. Technol. Lett.*, vol. 50, no. 8, pp. 2189–2191, 2008.

[9] S. Guo, L. Wu, K. W. Leung, and J. Mao, "Microstrip-fed differential dielectric resonator antenna and array," *IEEE Antennas Wireless Propag. Lett.*, vol. 17, no. 9, pp. 1736–1739, Sep. 2018.

[10] N. Mishra, S. Das, and D. Kumar V, "Beam steered linear array of cylindrical dielectric resonator antenna," *AEU – Int. J. Electron. Commun.*, vol. 98, pp. 106–113, Sep. 2018.

[11] A. Buerkle, K. F. Brakora, and K. Sarabandi, "Fabrication of a DRA array using ceramic stereolithography," *IEEE Antennas Wireless Propag. Lett.*, vol. 5, pp. 479–482, Nov. 2006.

[12] P. Bhartia, K. Rao, and R. Tomar, *Millimeter-Wave Microstrip and Printed Circuit Antennas* (Series Antennas and Propagation Library). Boston, MA, USA: Artech House, 1991.

[13] P. S. Hall and C. M. Hall, "Coplanar corporate feed effects in microstrip patch array design," *IEE Proc. H - Microw. Antennas Propag.*, vol. 135, no. 3, pp. 180–186, Jun. 1988.

[14] A. Rivera-Lavado *et al.*, "Design of a dielectric rod waveguide antenna array for millimeter waves," *J. Infrared Millim. Terahertz Waves*, vol. 38, no. 1, pp. 33–46, Jan. 2017.

[15] A. Rivera-Lavado *et al.*, "Planar lens-based ultra-wideband dielectric rod waveguide antenna for tunable THz and sub-THz photomixer sources," *J. Infrared Millim. Terahertz Waves*, vol. 40, no. 8, pp. 838–855, Aug. 2019.

[16] M. S. Abdallah, Y. Wang, W. M. Abdel-Wahab, and S. Safavi-Naeini, "Design and optimization of SIW center-fed series rectangular dielectric resonator antenna array with 45 linear polarization," *IEEE Trans. Antennas Propag.*, vol. 66, no. 1, pp. 23–31, Jan. 2018.

[17] W. M. Abdel-Wahab, Y. Wang, and S. Safavi-Naeini, "SIW hybrid feeding network-integrated 2-D DRA array: Simulations and experiments," *IEEE Antennas Wireless Propag. Lett.*, vol. 15, pp. 548–551, 2016.

[18] J. Lacik *et al.*, "Compact arrays fed by substrate integrated waveguides," in *Proc. IEEE-APS Topical Conf. Antennas Propag. Wireless Commun.*, Aug. 2014, pp. 448–451.

[19] F. Xu and K. Wu, "Guided-wave and leakage characteristics of substrate integrated waveguide," *IEEE Trans. Microw. Theory Techn.*, vol. 53, no. 1, pp. 66–73, Jan. 2005.

[20] K. Wu, Y. J. Cheng, T. Djerafi, and W. Hong, "Substrate-integrated millimeter-wave and terahertz antenna technology," *Proc. IEEE*, vol. 100, no. 7, pp. 2219–2232, Jul. 2012.

[21] A. S. Al-Zoubi, A. A. Kishk, and A. W. Glisson, "A linear rectangular dielectric resonator antenna array fed by dielectric image guide with low cross polarization," *IEEE Trans. Antennas Propag.*, vol. 58, no. 3, pp. 697–705, Mar. 2010.

[22] A. Al-Zoubi, A. Kishk, and A. W. Glisson, "Slot-aperture-coupled linear dielectric resonator array fed by dielectric image line backed by a reflector," in *Proc. IEEE Antennas Propag. Soc. Int. Symp.*, Jul. 2008, pp. 1–4.

[23] P. Bhartia and I. Bahl, *Millimeter Wave Engineering and Applications* (Series A Wiley-Interscience Publication). New York, NY, USA: Wiley, 1984.

[24] A. Lakshmanan and C. S. Lee, "A standing-wave microstrip array antenna," *IEEE Trans. Antennas Propag.*, vol. 59, no. 12, pp. 4858–4861, Dec. 2011.

[25] C. S. Lee, J. E. Brown, M. Ezzat, and S. Jeong, "Two-dimensional standing-wave microstrip array antenna," *Microw. Opt. Technol. Lett.*, vol. 59, no. 4, pp. 927–930, 2017.

[26] C. Dichtl, P. Sippel, and S. Krohns, "Dielectric properties of 3D printed polylactic acid," *Adv. Mater. Sci. Eng.*, vol. 2017, pp. 1–10, Jul. 2017.

[27] S. Zhang, C. C. Njoku, W. G. Whittow, and J. C. Vardaxoglou, "Novel 3D printed synthetic dielectric substrates," *Microw. Opt. Technol. Lett.*, vol. 57, no. 10, pp. 2344–2346, 2015.

[28] "ANSYS Simulation driven product development, HFSS." [Online]. Available: https://www.ansys.com/, Accessed on: Aug. 15, 2019.

[29] W. F. Richards, Microstrip antenna, in *Antenna Handbook*, Y. T. Lo and S. W. Lee, Eds., New York, NY, USA: Van Nostrand Reinhold, 1993.

[30] A. Petosa and S. Thirakoune, "Rectangular dielectric resonator antennas with enhanced gain," *IEEE Trans. Antennas Propag.*, vol. 59, no. 4, pp. 1385–1389, Apr. 2011.

[31] A. A. Qureshi *et al.*, "Template-based dielectric resonator antenna arrays for millimeter-wave applications," *IEEE Trans. Antennas Propag.*, vol. 65, no. 9, pp. 4576–4584, Sep. 2017.